CHARACTERIZATION OF ASYMMETRY IN MAGNETOACOUSTIC EMISSION BURST BY NUMERICAL PROCESSES

M. Namkung
NASA Langley Research Center
Hampton, VA 23681

J. P. Fulton and B. Wincheski
Analytic Services and Materials, Inc.,
Hampton, VA 23666

R. DeNale
Caderoc Division of Naval Surface Warfare Center
Annapolis, MD 21402

INTRODUCTION

It has been well known that the pattern of the magnetoacoustic emission (MAE) burst observed during the sweep over one half-cycle of the hysteresis loop becomes asymmetric depending on the strength of the magnetic domain wall-defect interaction and the state of residual stresses in a ferromagnet [1]. The ascending asymmetry due to the former has been observed at a very low frequency (.7 Hz) of applied AC magnetic field at a given amplitude [2]. The descending asymmetry due to uniaxial compressive stress has been typically observed at the AC applied magnetic field frequency of 20 Hz. The physical interpretation of both types of asymmetry has been well established [3]. It is, however, necessary to perform investigations of the dependence of asymmetry on externally controlled parameters such as the amplitude and frequency of the AC applied magnetic fields. The purpose of the present study is therefore to devise a mathematical means that describes the degree of asymmetry of the MAE burst and apply this scheme to investigate the AC magnetic field amplitude dependence of the asymmetry.

EXPERIMENTS AND NUMERICAL PROCESSING

Among the six low carbon samples used for the present study one has never been heat treated and its impact strength was estimated to be about 172.9 newton-meters (127.5 ft-Lbs.). The remaining five samples have been heat treated at 538^{o}C for 1, 5, 24, 50 and 100 hours and their impact strengths were estimated to be 73.9 (54.5), 20.3 (15.0), 12.9 (9.5), 8.8(6.5) and 6.8(5.0) newton-meters (ft-Lbs.) respectively. The detailed information on the sample preparation can be found elsewhere [4]. The basic elements of the MAE experimen-

tal control and data acquisition system can be also found in the previous papers [2,4].

The experiments were performed by controlling the amplitude of the sinusoidal current. The peak surface magnetic field was measured using a magnetic potentiometer originally invented by Chattock [5]. The magnetic potentiometer is a pickup coil wound on a cylindrical plastic rod formed in the shape of a semicircle. The diameter of the rod is about 4 mm and the radius of the semicircle is about 12 mm. A total of 450 turns of a 38 gauge wire was wound on the core. For calibration the potentiometer was located in the middle of a Helmholtz pair that applied an AC magnetic field of .7 Hz. The potentiometer output was integrated using an integrating fluxmeter in order to obtain the magnitude of the magnetic field. During the experiments, the potentiometer was positioned on top of the sample body and its output was integrated in the same way. The potentiometer measures the magnetic field strength just above the sample surface, but at some selected points in time the tangential component of magnetic field just above the sample surface is identical to that of the field just under the surface. To measure the peak amplitude of the surface magnetic field at these points in time the integration was necessary as explained in the following.

The appropriate boundary condition involving the magnetic fields at an interface is

$$\hat{n} \times (\vec{H}_2 - \vec{H}_1) = \frac{4\pi}{c}\vec{K}$$

where $\vec{H}_2$ is the magnetic field right outside the sample, $\vec{H}_1$ is the field right inside the sample, $\hat{n}$ is a unit vector normal to the sample surface and $\vec{K}$ is the surface current density. The magnitude of the left-hand-side of the above expression is the difference between the tangential components of the two magnetic fields at the interface. Both magnetic fields can be approximated to be parallel to the surface and the longer axis of the sample, and the direction of $\vec{K}$ is perpendicular to these fields. The surface current $\vec{K}$ exists due to the eddy currents generated and is proportional to $-\partial\phi/\partial t$ where ϕ is the total magnetic flux in the sample. The total magnetic flux $\phi(t)$ is in phase with the magnetic field $\vec{H}(t)$. Since the output of the potentiometer is also proportional to $\partial H/\partial t$, integration of the output will shift its peak to the position in time where $-\partial\phi/\partial t = 0$ and at that moment $H_{1t} = H_{2t}$. Fig. 1 shows the tangential component of the peak surface magnetic field measured as a function of amplitude of the function generator signal that controlled the power supply.

Due to the random nature in the annihilation/regeneration cycles of the magnetic domain, the MAE waveforms observed during the successive cycles over the hysteresis loops are not exactly reproducible. To enhance the statistically stable results it is therefore necessary to average the MAE waveforms over a certain number of hysteresis loops. A

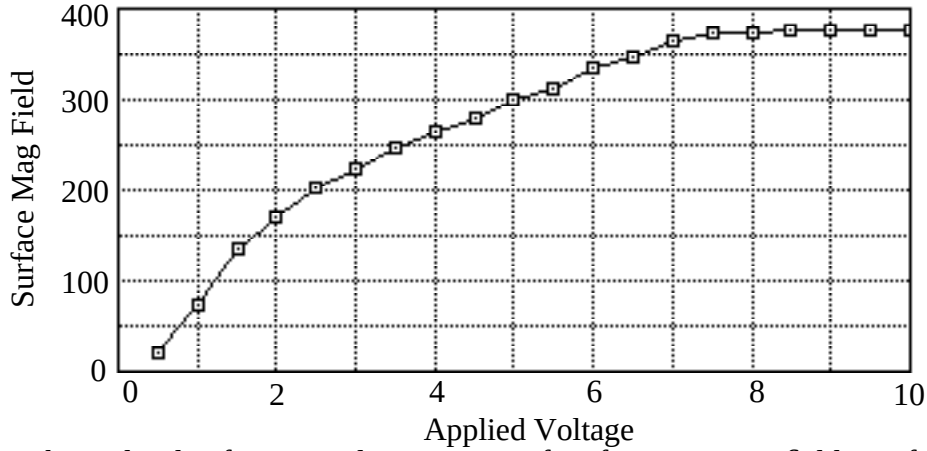

Fig. 1. Peak amplitude of tangential component of surface magnetic field as a function of the control sine wave amplitude input to the power supply/amplifier.

series of separate experiments has shown that the average over 50 one-half-cycles of the hysteresis loop provides sufficient accuracy.

The first step of numerical processing is to construct a normalized distribution from the rectified and averaged MAE spectrum as follows:

$$g(t_i) = \frac{h(t_i)}{\sum_j^N h(t_i)}$$

where $h(t_i)$ represents the average rectified individual pulses of the raw MAE spectrum and N is the total number of pulses in burst. The function $g(t_i)$ is smoothed and then the first moment of the distribution is obtained as

$$E(t_i) = \mu_t = \sum_i^N t_i g(t_i)$$

which is the weighted average of the point t_i. The next step is to obtain the variance which is defined as

$$E(t-\mu_t)^2 = \sigma_\tau^2 = \sum_i^N (t_i-\mu_t)^2 g(t_i)$$

which is a measure of the spread of $g(t)$ about its mean. The skew is then defined as follows:

$$Sk_t = \sum_i^N \frac{(t_i-\mu_t)^3 g(t_i)}{(\sigma_\tau^2)^{\frac{3}{2}}}$$

which is a measure of the skewness of the MAE burst after rectification, averaging and smoothing processes.

RESULTS AND DISCUSSION

Fig. 2 shows the results obtained at a driving amplitude of 5.0 V for the sample heat treated for one hour. The figure displays the induction pickup coil output and two raw MAE spectra for one half-cycle of the hysteresis loop. Clearly, the two spectra obtained in the repeated measurements with the same sample under identical experimental conditions show somewhat different features. Fig. 3 shows the results of the averaged induction pickup coil output and the rectified, averaged MAE spectrum over 3 half-cycles. Fig. 4 shows the results of the rectified and averaged MAE spectrum for 100 half-cycles for the same sample and under the same conditions as Fig. 3.

The results of Fig.4 show that, by averaging the MAE spectra over a sufficient number of half-cycles, one can obtain a fairly smooth envelope function of the rectified MAE spectrum. Comparing with the results of Fig. 3, it is apparent that the noise band in Fig. 4 is seen to be dramatically reduced. This is further evidence of the random nature involved in the. domain wall annihilation/regeneration process. Averaging only 3 half-cycles the total number of MAE events is not sufficient for a fair distribution among the channels of the digital scope resulting in a broad noise bandwidth. As more MAE bursts are averaged all the channels receive a fair share of MAE events resulting in a narrow noise bandwidth of the spec-

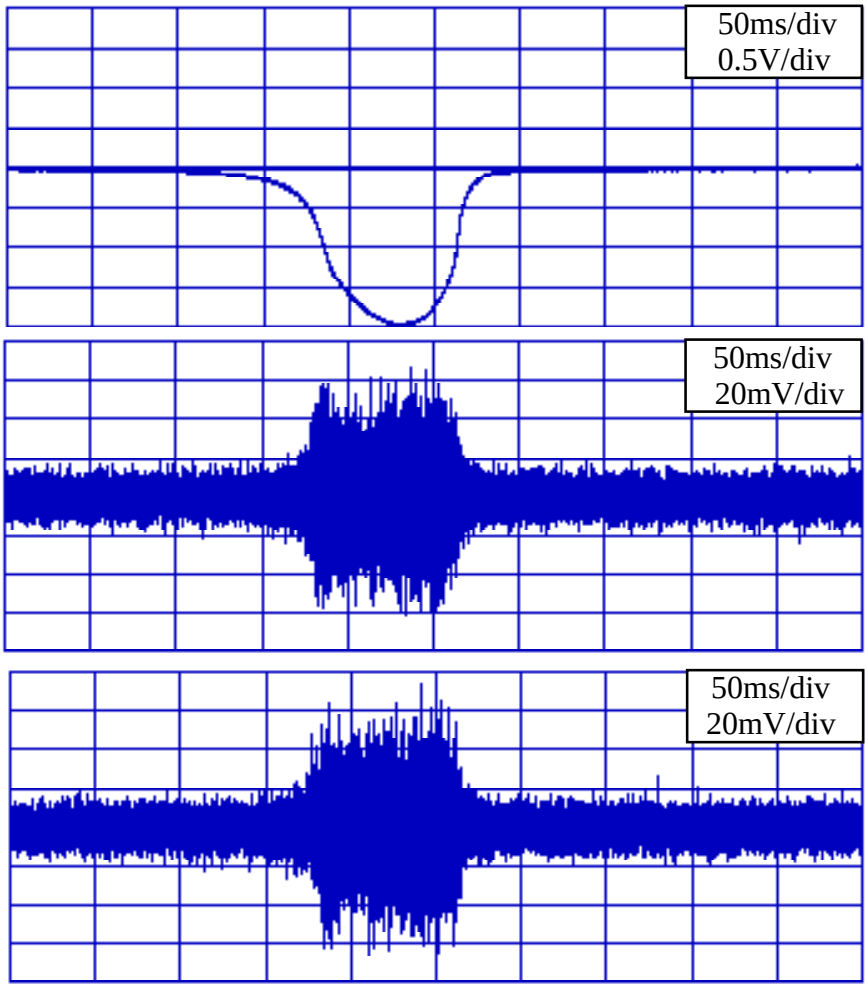

Fig. 2 Results of induction pickup coil output (upper trace), and raw MAE spectra obtained at different times with the sample heat treated for 1 hr. at a control sine wave amplitude of 5.0 V (middle and lower traces).

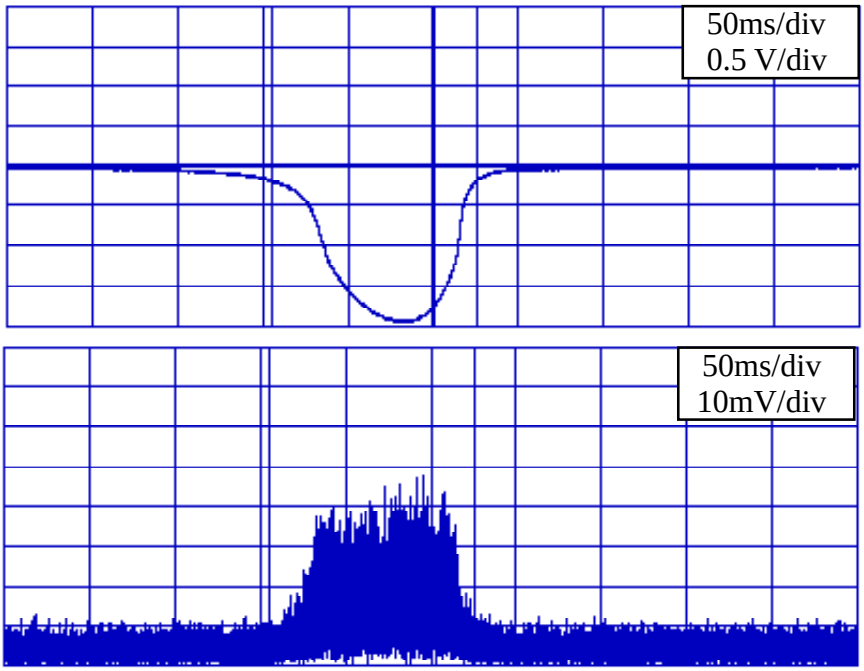

Fig. 3. Results of the induction pickup coil output, and rectification and averaging of the MAE spectra of 3 half-cycles under the same experimental conditions of Fig.2.

trum. The skew was then computed from the final spectrum of Fig. 4.

Fig. 5 shows the results of the averaged pickup coil output and the rectified, averaged spectrum of 100 half-cycles at 5.0 V driving sine wave amplitude obtained with the sample heat treated for 50 hours. The difference between the results of Fig. 4 and Fig. 5 is clear and is easily explained based on the strength of the domain wall-defect interaction. At .7 Hz the AC applied magnetic field frequency is low enough to saturate the sample. This is evident from the fact that there exists a long dead time between two successive pickup coil signals or MAE bursts. As the total magnetic induction is reduced from the saturation value, the magnetic domain walls execute the return trip towards the positions of the original equilibrium configuration. The sharp peak of Fig. 4 is due to the sudden motion of 90^o domain walls over the major potential barriers. The domain wall-defect interaction strength, however, depends on many different factors such as the mutual geometrical properties of domain walls and grain boundaries, the structural properties of grain boundaries, grain size and so on. Hence, it is relevant to say that each specimen has it own unique distribution function of the domain wall-defect interaction strength.

Under a given rate of change in the magnetic state of the system, the 90^o domain walls with an interaction strength below a certain level will execute the motion over the major potential barriers while the remaining 90^o domain walls remain pinned until a sufficient driving force becomes available. It must be noted that the location of this first sub-peak occurs prior to H = 0 which suggests that only the 90^o domain walls of high mobility are involved in this process. There will be a smaller fraction of 90^o domain walls of high mobility in the sample heat treated for 50 hours which is reflected in the much smaller initial peak seen in the MAE spectrum of Fig. 5. After the occurrence of the initial peak the motion of the remaining 90^o domain walls begins, resulting in a broad second peak as shown both in Figs. 4 and 5.

The induction pickup coil output shown in Fig. 2 and Fig. 3 are essentially identical while the MAE spectra of the corresponding cases show an obvious difference. This clearly supports the well known assumption that the change in total magnetic flux is mainly due to the motion of 180^o domain walls because they are relatively free to move, whereas the generation of MAE is mainly caused by the motion of 90^o domain walls due to their intrinsic involvement in the magnetostriction. In the domain wall motion region of the hysteresis loop, however, these two types of magnetic domain walls are coupled together which means the pinned 90^o domain walls bend just as pinned dislocations to allow the continuous motion of 180^o domain walls.

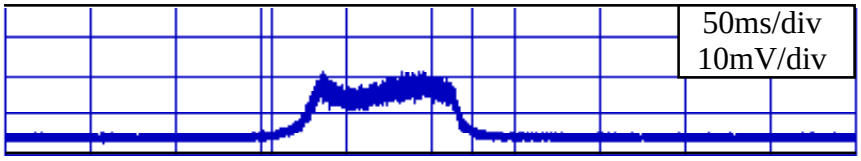

Fig. 4. Results of rectification and averaging of the MAE spectra over 100 half-cycles obtained under the same experimental conditions of Figs. 2 and 3.

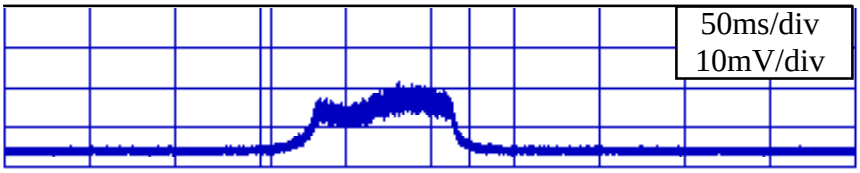

Fig. 5. Results of rectification and averaging of MAE spectra over 100 half-cycles obtained with the samples heat treated for 50 hours under the same experimental conditions.

The initial results of the applied magnetic field amplitude dependence of skew obtained by averaging over 50 half-cycles of rectified MAE spectra are shown in Fig. 6. In this figure it is clearly seen that the skew is generally a decreasing function of applied magnetic field amplitude. The functional curve obtained with the untreated sample starts out with a positive skew value, which means a larger first sub-peak in the MAE burst, and slowly decreases towards negative values due to the growth in the overall amplitude of the second sub-peak in the burst.

Such a dependence observed with the untreated sample is easily understood. As the magnitude of the applied field is reduced from its maximum to zero, the magnetic domain walls move towards their positions in the original equilibrium state. During this process, the driving force is due only to the demagnetization field which exists even though the magnetic system was designed to minimize such effects by forming closed magnetic circuits. The increase in the amplitude of applied field pushes the 90^o domain walls further away from the their original positions. Hence, fewer 90^o domain walls participate in the initial return trip induced by the demagetization field due to an increased probability of pinning of the 90^o domain walls away from their equilibrium positions. The fraction of 90^o domain walls contributing to the formation of the first or second sub-peaks of the MAE burst is therefore determined by the amplitude of the applied magnetic field under given conditions of the system.

As the heat treatment increases, the degree of embrittlement is generally enhanced and the potential barriers at the grain boundaries becomes more effective in resisting the motion of 90^o domain walls, which is equivalent to saying that the strength of the domain wall-defect interaction is increased. Thus, the demagnetization field-induced return trip becomes more and more difficult as the degree of embrittlement is enhanced causing an increase in the fraction of 90^o domain walls participating in the formation of the second sub-peak in the burst. The skew therefore becomes more negative as the heat treatment time increases. This explains the down-shift of the curves for the more embrittled samples in Fig. 6. The skew curves in Fig. 6 were obtained from repeated measurements without any significant time delay between measurements taken at different field strengths. We noticed that if the tests were duplicated on the same sample, shortly after obtaining a set of results, the skew values

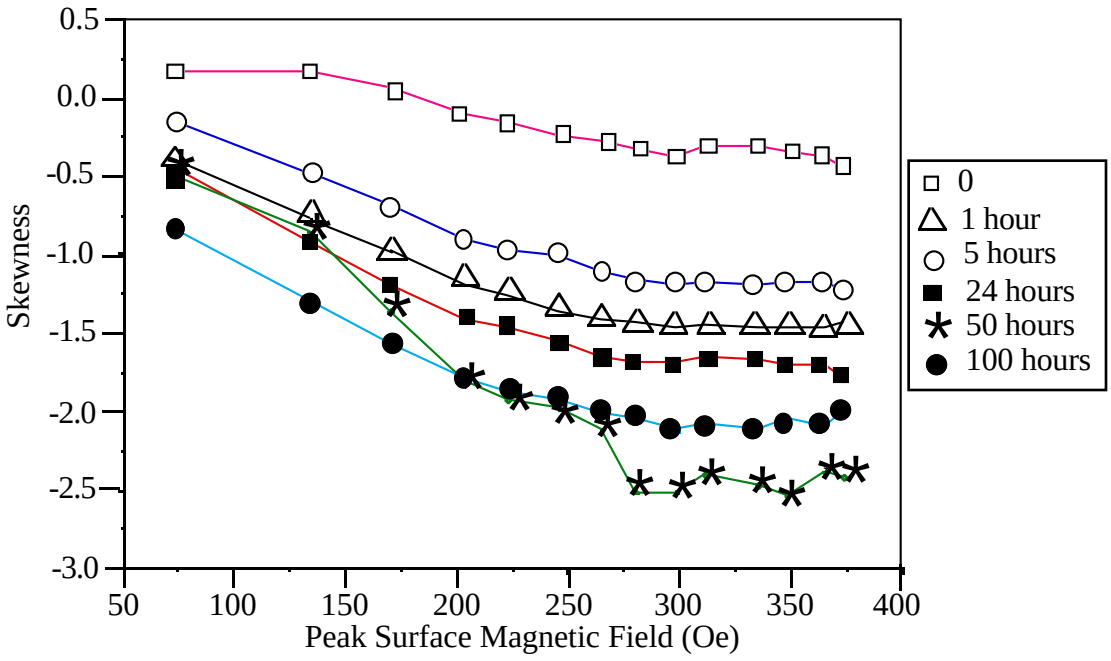

Fig. 6. Results of the applied magnetic field amplitude dependence of the skewness of the MAE burst obtained with the untreated and five heat treated samples.

changed. This is due to a time dependence involved in the magnetic system of the samples and an explanation of the phenomenon is presented later in this section. Each curve in Fig. 6 was obtained by averaging the first 50 MAE spectra after each sample had been demagnetized and left undisturbed for a minimum of two days.

The curves of the samples heat treated for 50 and 100 hours cross each other which appears to be in contradiction to the explanations given above. Such results were, however, expected based on the previous experimental results. The initial results of MAE pulse height analysis and remanence clearly indicated that the sample heat treated for 50 hours actually has a higher interaction strength than that heat treated for 100 hours [4]. More recent results of pulse height analysis also showed the same trend [2]. Hence, if we assume that the 50 hour heat treated sample is actually more embrittled, the crossing between the two curves can be explained.

As the domain wall motion-resisting potential barriers becomes stronger, it takes a higher applied magnetic field for 90^o domain walls to jump over these barrier peaks. At a smaller AC applied magnetic field amplitude, therefore, the motion of the majority of the 90^o domain walls is confined between two major potential barriers and within this limit their motion is relatively free. This means that between the two highly embrittled samples, the one with higher domain wall-defect interaction strength may allow a freer motion of 90^o domain walls at a relatively small amplitude of the applied AC magnetic field allowing more 90^o domain walls to participate in the formation of the first sub-peak of the MAE burst. As the applied magnetic field amplitude increases, the range of 90^o domain wall motion extends over the major barrier peaks. The demagnetization field-induced return trip, which causes the first sub-peak, becomes more difficult. Beyond a certain level of AC field amplitude in a more embrittled sample more 90^o domain walls participate in the formation of the second sub-peak and the skew curves cross each other.

Fig. 7 shows the skew values of the sample heat treated for 50 hours obtained by averaging the MAE spectra of the first 50 half-cycles and the next 75 half-cycles after the sample had been demagnetized and left undisturbed for two days. The latter curve apparently shows a smooth decrease in the skewness with the initial values shifted towards the negative side indicating the motion of the 90^o domain walls at the low applied field magnitudes is

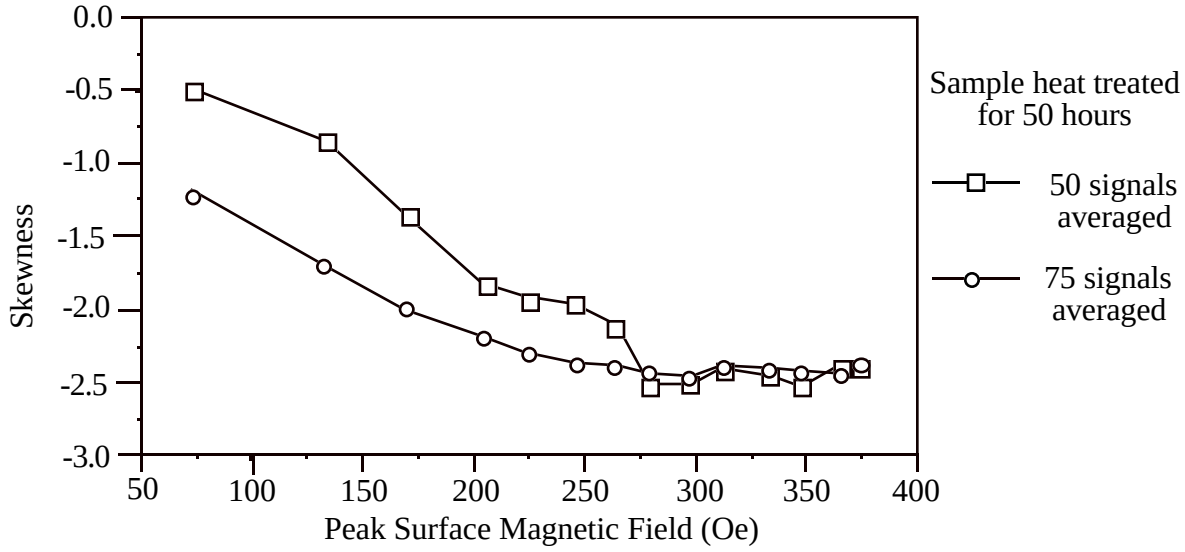

Fig. 7. Two curves of the skewness obtained for the first 50 and the next 75 half-cycles of hysterisis loops of the 50 hour heat treated sample after it was demagnetized and left undisturbed for two days.

extended upon the repetition of hysteresis cycles. The results of the same measurements performed with the two samples heat treated for 5 and 24 hours show that the time dependent effect is less pronounced in the less embrittled samples.

Any ferromagnet containing a certain amount of interstitial impurities is known to show a magnetic after-effect to some degree [6]. This is based on the occupational probabilities of the impurities among crystallographically equivalent but magnetically inequivalent octahedral or tetrahedral sites. It is well known that a solid solution of carbon in a iron-like ferromagnet, the case of the samples used in the present experiment, causes the magnetic after-effect.

The time dependence of skewness shown in Fig. 7 is the maximum limit so far discovered during the experiments, but it must be confirmed by a more systematic long term investigation. A time dependent effect has been previously found in the magnetoacoustics experiment where the pattern of $\Delta f(B)/f$ changed during the repeated measurements and about three hours of relaxation time was needed to recover the initial pattern of the curves [6]. Such a time dependence observed in the magnetoacoustics experiments is assumed to be of the same origin as that observed in the present experiments. More details are, however, yet to be studied.

SUMMARY

A new numerical processing scheme was applied to describe the skewness of the MAE burst in an unembrittled low carbon sample and five samples of the same chemical composition but with varying degrees of embrittlement. The skewness was seen to decrease monotonically upon the increase in the applied AC magnetic field amplitude which was explainable based on domain wall motion along the hysteresis loop. The skew vs. amplitude curve was also time dependent, most probably due to the effects of solid solution of carbon. More details are, however, unavailable at present.

REFERENCES

1. M. Namkung, W. T. Yost, D. Utrata and R. DeNale, in *Review of Progress in Quantitative NDE*, Vol 9B, edited by D. O. Thompson and D. E. Chimenti (Plenum Press, New York, 1990), p. 1911.

2. M. Namkung, R. DeNale and R. G. Todhunter, in *Review of Progress in Quantitative NDE*, Vol. 10B, edited by D. O. Thompson and D. E. Chimenti (Plenum Press, New York, 1991), p. 2007.

3. M. Namkung, D. Utrata and R. DeNale, in *Proc. of IEEE Ultrasonics Symp*. (1990), Vol. 2, p 983.

4. S. G. Allison, W. T. Yost, J. H. Cantrell and D. F. Hasson, in *Review of Progress in Quantitative NDE*, Vol. 7B, edited by D. O. Thompson and D. E. Chimenti (Plenum Press, New York, 1991), p. 1463.

5. L.F. Bates, Modern Magnetism (Cambridge University Press, 1963).

6. M. Namkung and D. Utrata, in *Review of Progress in Quantitative NDE*, Vol. 7B, edited by D. O. Thompson and D. E. Chimenti (Plenum Press, New York, 1991), p. 1429.